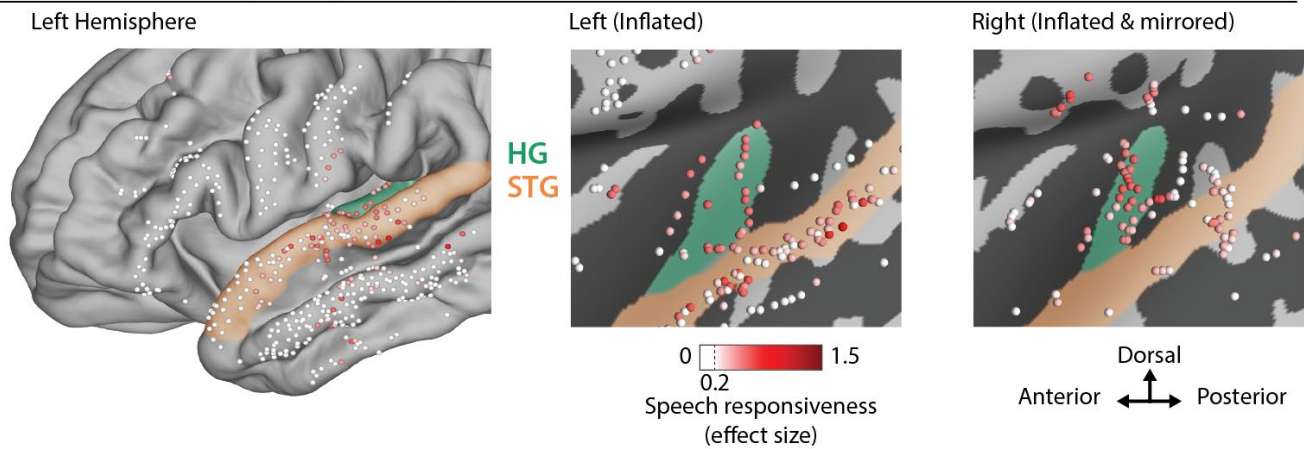


Supplementary materials

a Electrode coverage and speech responsiveness



b Speaker Selectivity Index (SSI)

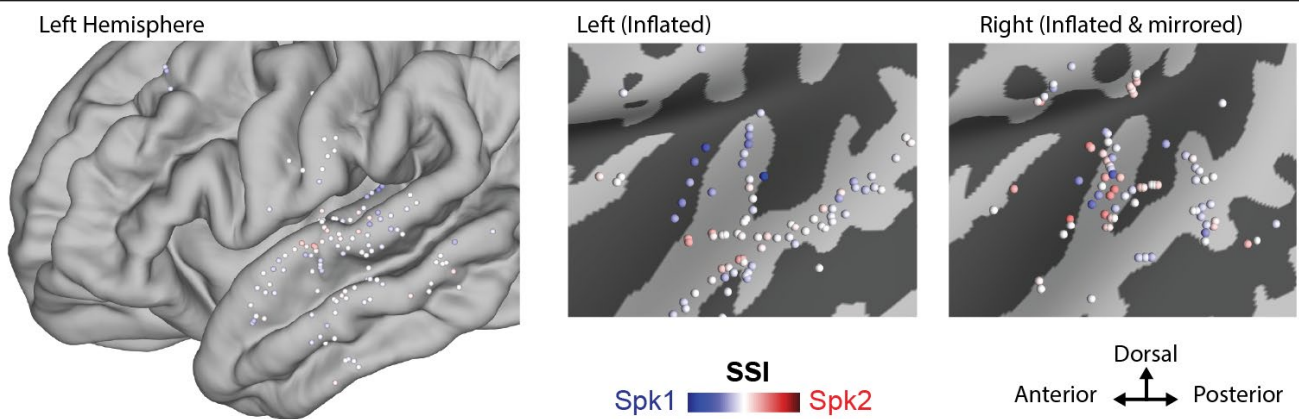


Figure S1, related to Figure 1. (a) Electrode coverage and speech responsiveness from all electrodes. **(b)** The anatomical distribution of the speaker-selectivity index (SSI). Only electrodes that were significantly responsive to speech (Cohen's $D > 0.2$) are shown. See Fig. 1 for a description of the anatomy.

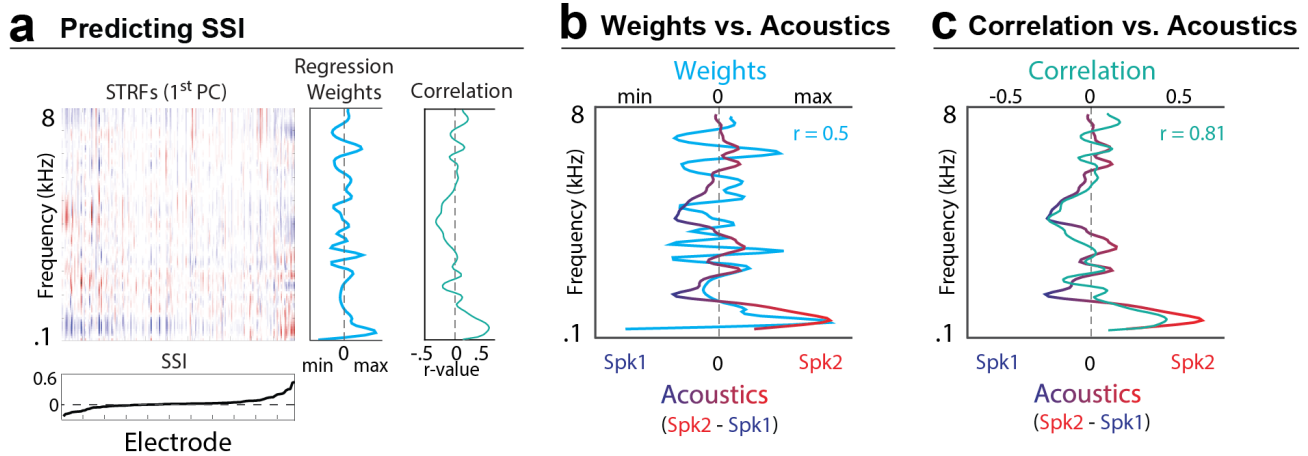


Figure S2, related to Figure 2. Predicting the speaker-selectivity index (SSI). **(a)** The spectral response profile for each electrode (1st PC of their STRFs) sorted according to their SSI (bottom panel). Plotted on the right are the regression weights applied to each frequency band that were learned to predict the SSI. The correlation between each frequency band and the SSI is also plotted. **(b)** A comparison of the regression weights with the difference in the acoustics of Spk1 and Spk2. **(c)** A comparison of the correlation vector with the difference in the acoustics of Spk1 and Spk2.

Speech Responsiveness vs. AMI

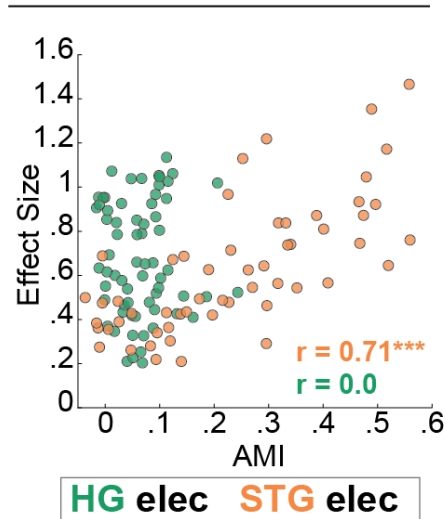
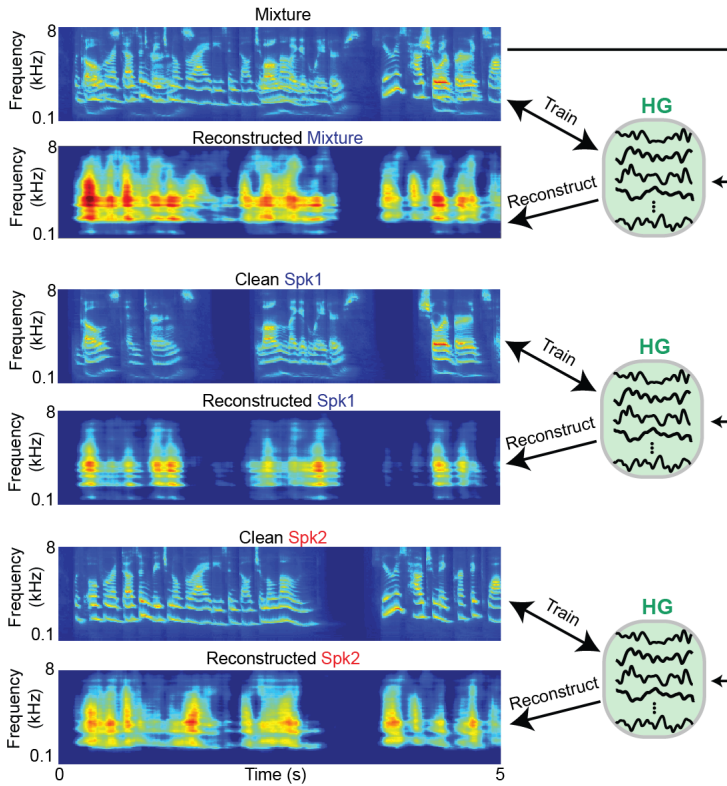


Figure S3, related to Figure 3. Comparing speech responsiveness (effect size: speech vs. silence) with the AMI. The large correlation in STG ($r = 0.71$, $p < 0.001$) but not in HG ($r = 0$) is probably because our measure of attention is based on the correlation between the multi and single-talker responses and is affected by the signal-to-noise ratio (SNR) of the recording at each electrode. In HG, sites that are extremely responsive to speech can still be modulated by attention. However, even if a site in STG is modulated by attention, we are limited in measuring it due to the signal quality.

a Training linear decoders to separate speakers in HG



b Speakers are linearly separable in HG

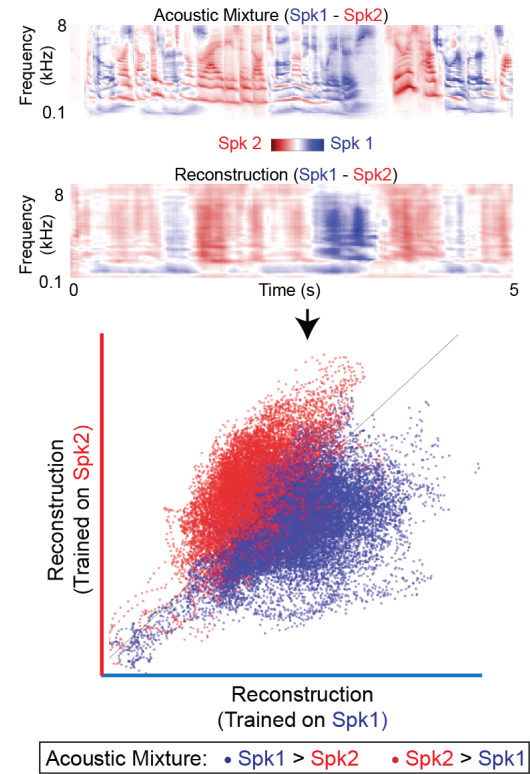
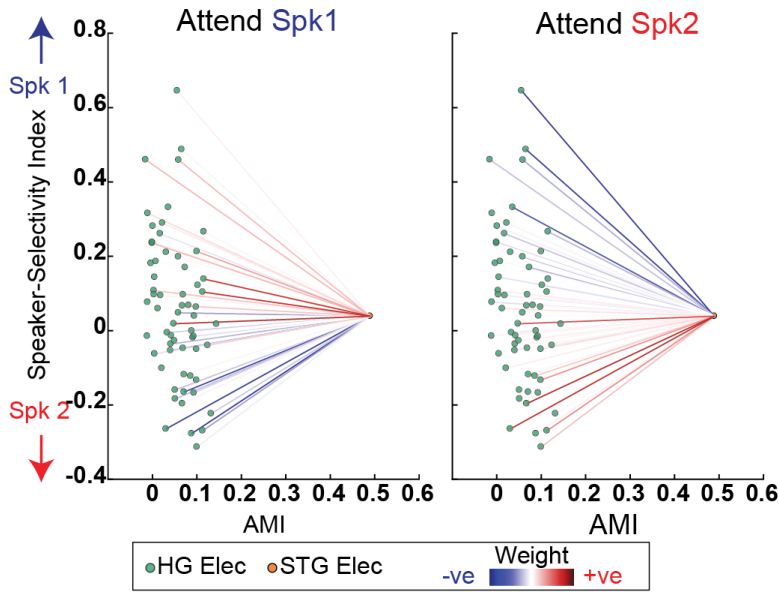


Figure S4, related to Figure 6. Extended visualization of speaker separability in HG (cf. Fig. 5). **(a)** Top panel: the mixture can also be reconstructed from the responses in HG. Middle and bottom panels: same as in Fig. 5a but including a comparison with the clean spectrograms of Spk1 and Spk2. **(b)** Same as Fig. 5b but including a visualization of the clean and reconstructed spectrograms (the difference between Spk1 and Spk2) to illustrate how the colors are assigned to each time-frequency bin in the scatter plot (bottom panel).

a HGRF Weights (example STG elec)



b Comparison with AMI

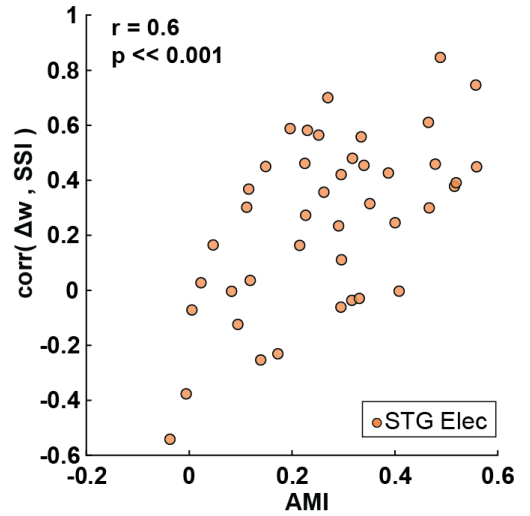
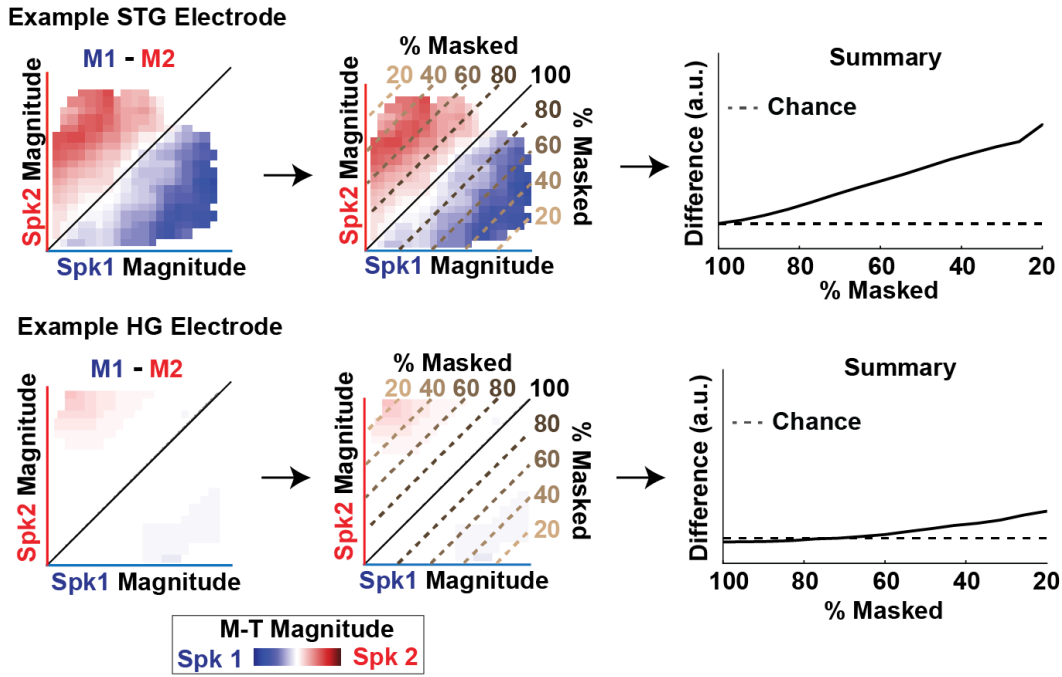
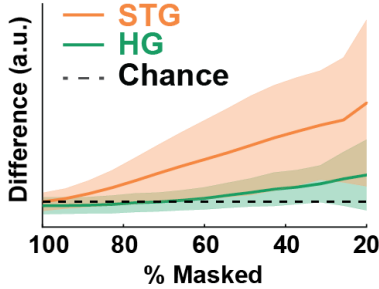


Figure S5, related to Figure 7. (a) Extended visualization of the weight dynamics from HG to STG in the multi-talker condition (cf. Fig. 6c). For an example electrode in STG (orange dot), the plot shows the weights applied to each HG electrode (green dots) when Spk1 (left panel) and Spk2 (right panel) are attended. Blue (red) indicates a positive (negative) weight. **(b)** The AMI for each STG electrode (orange dots) plotted against the correlation between the change in weights and SSI for the HG electrodes. The positive correlation ($r = 0.6$) indicates that the sites that are more strongly modulated by attention show the largest change in weights with attention.

a Effect of Relative Speaker Magnitude



b Anatomical Comparison



c Linear Fit to Energetic Masking Curves

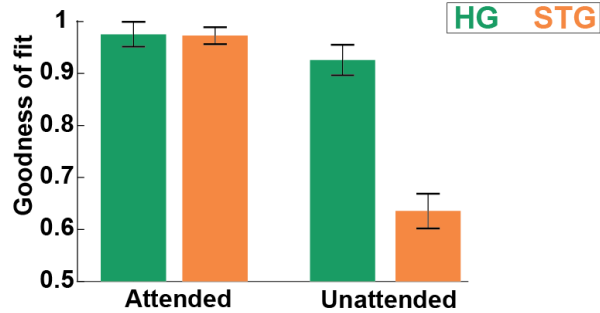
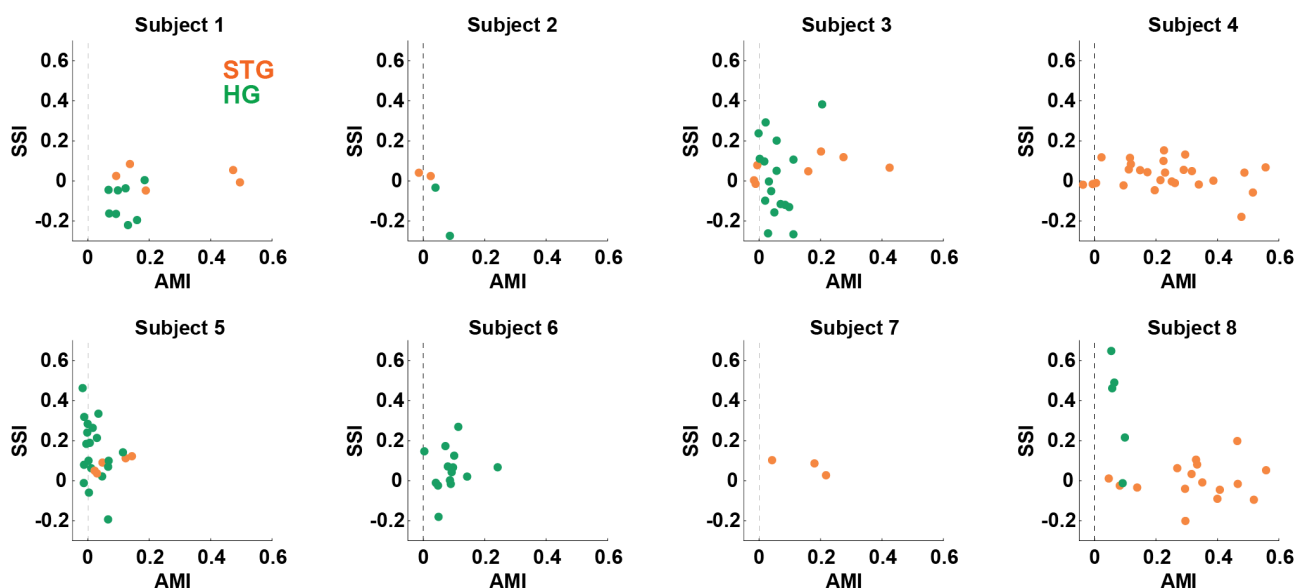


Figure S6, related to Figure 5. (a) Alternative method of visualizing energetic masking (cf. Fig. 8). For the same example electrodes in STG and HG, the difference between M1 and M2 matrices is obtained. Then, by averaging along the diagonals of this matrix (where each diagonal represents the relative amount masking, i.e., 0 to 100% masked), we can summarize the 2D matrix into a 1D line, indicating the amount of attentional modulation for each level of masking. A chance level of attentional modulation was calculated by randomly shuffling the data. **(b)** The same analysis applied to the population of responses in HG and STG. Solid lines and shaded regions indicate the mean and standard deviation, respectively. This analysis reveals that most sites in HG (85%) are slightly modulated by attention but at only low levels of energetic masking. **(c)** Goodness of fit (0-1) for linear fits to the energetic masking curves in Fig. 8c and d. This analysis shows that HG linearly represents both attended and unattended speakers, whereas STG linearly represents the attended speaker only.

a AMI vs. SSI for individual subjects



b AMI vs. SSI (comparing left versus right hemisphere)

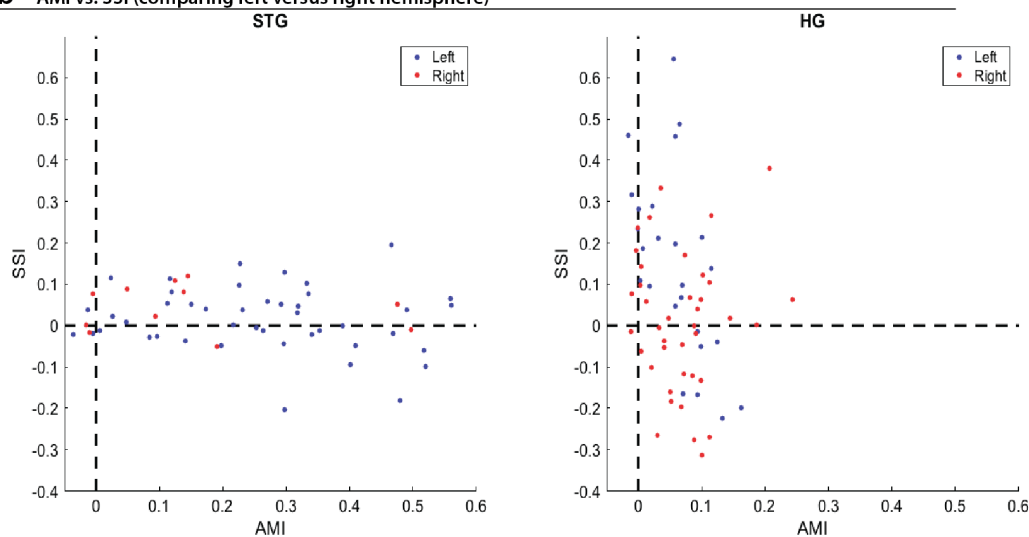


Figure S7, related to Figure 4. (a) The attentional modulation index (AMI) versus the Speaker-Selectivity Index (SSI) for each individual subject. Subjects 4 and 8 had high density ECoG grids implanted over the left hemisphere with coverage of STG (orange). Subject 8 also had a depth electrode implanted in HG (green). The remaining subjects had depth electrodes with varying amounts of coverage of HG and STG. **(b)** Hemisphere comparison. The attentional modulation index (AMI) versus the Speaker-Selectivity Index (SSI) across all subjects, comparing the left-hemisphere (blue) and right-hemisphere (red).

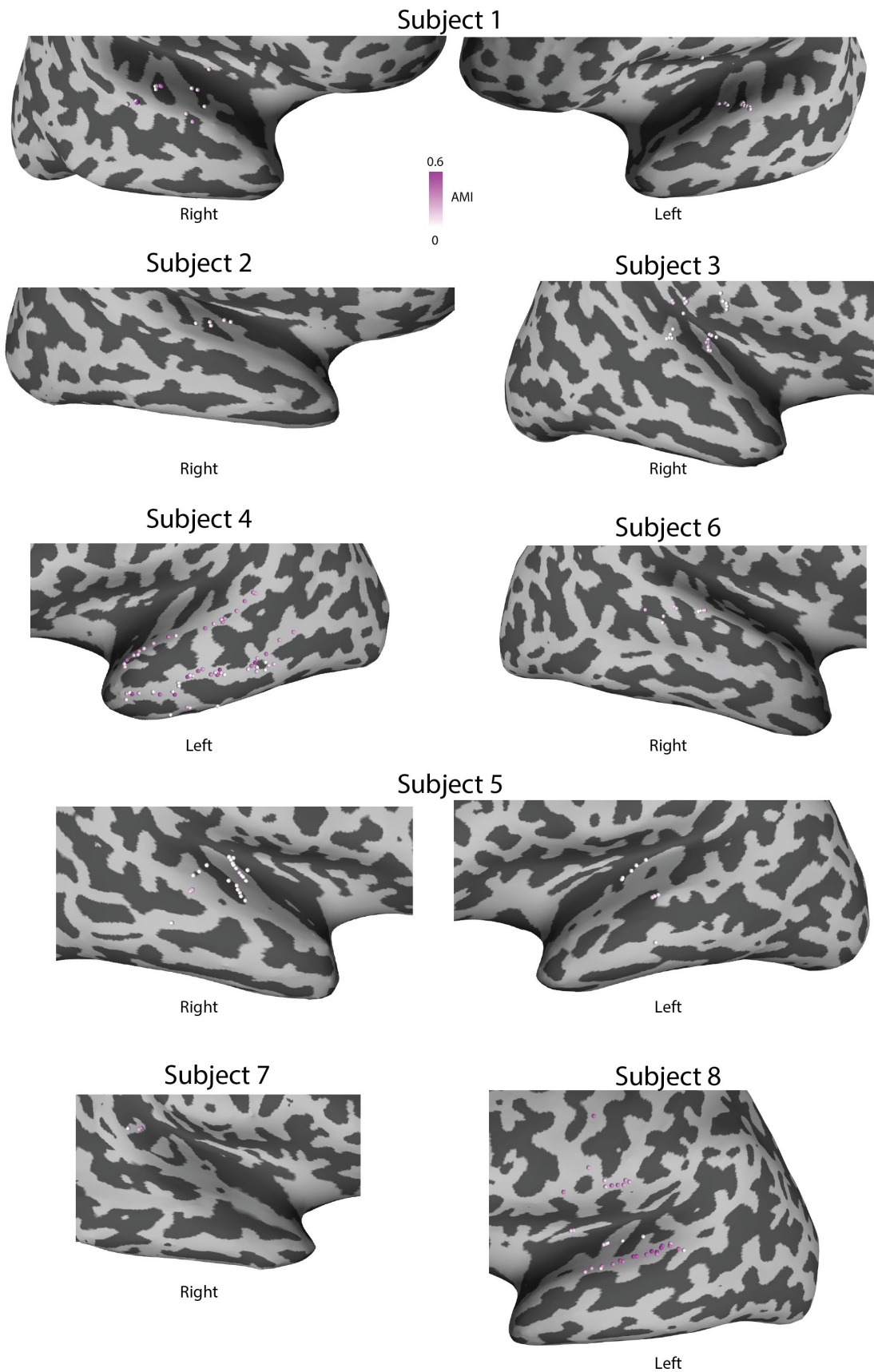


Figure S8, related to Figure 3. The AMI (magenta) for each subject, plotted on individual inflated cortices.